COVER SHEET

Electron paramagnetic resonance, optical absorption and IR spectroscopic studies of the sulphate mineral apjohnite

S. Lakshmi Reddy [1], G. Siva Reddy [2], D.L. Wain[3], W.N. Martens[3], B. Jagannatha Reddy[3] and R. L. Frost [3]•

1. Dept. of Physics, S.V.D. College, Kadapa 516 003, India.

2. Dept. of Chemistry, S.V.U.P.G. Centre, Kadapa 516 003, India

3. Inorganic Materials Research Program, Queensland University of Technology, 2 George Street, Brisbane, GPO Box 2434, Queensland 4001, Australia

Abstract

Apjohnite, a naturally occurring Mn-bearing pseudo-alum from Terlano, Bolzano, Italy has been characterized by EPR, optical, IR and Raman spectroscopy. The optical spectrum exhibits a number of electronic bands around 400 nm due to Mn(II) ion in apjohnite. From EPR studies the parameters derived, g = 2.0 and A = 8.82 mT confirm $MnO(H_2O)_5$ distorted octahedra. The presence of iron impurity in the mineral is reflected by a broad band centered around 8400 cm^{-1} in the NIR spectrum. A complex band profile appears strongly both in IR and Raman spectra with four component bands around 1100 cm^{-1} due to the reduction of symmetry for sulphate ion in the mineral. A strong pair of IR bands at 1681 and 1619 cm^{-1} with variable intensity is a proof for the presence of water in two states in the structure of apjohnite.

Keywords: Apjohnite; Pseudo-alum; Optical absorption spectrum; EPR; Near-infrared spectroscopy; IR and Raman spectroscopy

• Author to whom correspondence should be addressed (r.frost@qut.edu.au)
P: +61 7 3864 2407 F: +61 7 3864 1804

1. Introduction

Alums have the general formula $RM(SO_4)_2.12H_2O$ or $R_2SO_4.M_2(SO_4)_3.24H_2O$, where M = trivalent aluminum, iron, chromium, manganese, cobalt, gallium, rhodium or thallium and R = monovalent sodium, potassium, ammonia, lithium, or cesium. The alums form two groups namely kalinite or potash alum and the halotrichite mineral series. The halotrichite mineral series alums are pickeringite, halotrichite, bilinite, apjohnite, dietrichite and wupatkiite. Apjohnite belongs to pseudo-alums. Raman microscopy of apjohnite has been reported [1].

Apjohnite mineral used in the present study originates from Terlano, Bolzano, Italy. Chemical analysis was reported and yields the calculated crystallochemical formula $(Mn_{0.64}\ Mg_{0.28}\ Zn_{0.06}\ Fe_{0.02})\ Al_2\ (SO_4)_4.22H_2O$ [2]. Its crystal structure is monoclinic with space group $P2_1/c$. The lattice constants are a = 0.6198(2), b = 2.4347(4), c = 2.1266(4) nm, β = 100.28(3)° and Z = 4. In the crystal structure four crystallographically independent sulphate ions are present. One acts as a unidentate ligand to the M(II) ion, and the other three are involved in complex hydrogen bond arrays involving coordinated water molecules to both cations and to the lattice water molecules. The SO_4 tetrahedra, $Al(H_2O)_6$ octahedra, and $MnO(H_2O)_5$ octahedra are connected by a H bonding system; the only direct connection between polyhedra is by sharing of an O between S(4) and Mn [3-4].The effect of cation and its symmetry on spectral properties can be explained by crystal field theory. Octahedral coordination of Mn(II) in apjohnite has five valence electrons occupying three in t_{2g} and two in e_g orbitals and $^6A_{1g}$ forms the ground state. The transitions of $MnO(H_2O)_5$ groups are spin forbidden. However visible spectrum shows sharp bands near 400 nm (25000 cm^{-1}) for all Mn-complexes [5,6].

IR spectra of alums based on one monovalent and one trivalent cation have been published [7]. Ross reported the interpretation of the infrared spectrum of potassium alum as ν_1, 981 cm^{-1}; ν_2, 465 cm^{-1}; ν_3, 1200, 1105 cm^{-1}; ν_4, 618 and 600 cm^{-1} for $(SO_4)^{2-}$. Water stretching modes were reported at 3400 and 3000 cm^{-1}, bending modes at 1645 cm^{-1}, and librational modes at 930 and 700 cm^{-1} [8]. The Raman spectra of synthetic alums have been extensively studied [9,10]. However, little attention has been paid on the study of the spectra of naturally occurring, Mn bearing alum-apjohnite. So far for this mineral no studies of the optical absorption, electron paramagnetic resonance and IR studies have been reported. Therefore in this work we report the electron paramagnetic resonance, optical absorption, NIR and IR spectroscopy of apjohnite and review the Raman data reported on natural pseudo-alums [1].

2. Experimental Studies

A white sample of apjohnite from Terlano, Bolzano, Italy is used in the present work. EPR spectra of the powdered sample were recorded at room temperature (RT) on JEOL JES-TE100 ESR spectrometer operating at X-band frequencies (ν = 9.1-9.5 GHz), having a 100 KHz field modulation to obtain a first derivative EPR spectrum. DPPH with a g value of 2.0036 is used for g factor calculations.

Varian Cary 3 UV-Visible spectrophotometer, equipped with Diffuse Reflectance Accessory (DRA) was employed to record the electronic spectrum of the sample in the region between 200 and 900 nm. The diffuse reflectance measurements were converted into absorption (arbitrary units) using the Kubelka-Munk function ($f(R_\infty) = (1- R_\infty)^2/2R_\infty$). Data manipulation was performed using Microsoft Excel. The details of experimental techniques were followed as reported [11]. Raman microprobe spectroscopy consists of Renishaw 1000 Raman microscope system in conjunction with monochromator, a filter system and a Charge Coupled Device (CCD) was employed. He-Ne laser was used to excite the sample. Small crystals of the apjohnite mineral were used to record the Raman spectrum in the range 4000 to 100 cm^{-1}. Other details of the experimental technique have already been reported [12,13].

Spectroscopic manipulations such as baseline adjustment, smoothing and normalization were performed using the Spectracalc software package GRAMS (Galactic Industries Corporation, NH, USA). Band component analysis was undertaken using the Jandel "PEAKFIT" software package which enabled the type of fitting function to be selected and specific parameters to be fixed or varied accordingly. Band fitting was carried out using a Lorentz-Gauss cross product function with a minimum number of component bands used for the fitting process. The Lorentz-Gauss ratio was maintained at values greater than 0.7 and fitting was undertaken until reproducible results were obtained with squared correlations of r^2 greater than 0.9975.

3. Results and analysis

3.1. Electron paramagnetic resonance analysis

If manganese is present in the mineral, electron paramagnetic resonance will show its presence by a six line pattern in the EPR spectrum. Fig.1 shows the EPR spectrum of polycrystalline apjohnite mineral observed at room temperature. It is well known that in the transition metal ion EPR studies, Mn(II) is easily observable at room temperature, even if present in minute levels, compared to other ions. Fig. 2 clearly indicates the presence of Mn(II) in the sample. It contains a strong sextet at the centre of the spectrum corresponding to the electron spin transition +1/2> to -1/2>. Generally, in most of the cases, the powder spectrum is characterized by a sextet, corresponding to this transition. The other four transitions, corresponding to ±5/2> ↔ ±3/2> and ±3/2>↔ ±1/2> are not seen due to their high anisotropy in D. The observed g = 2.0 and D =33 mT. This value of D indicates a considerable amount of distortion around the central metal ion. From the powder spectrum of the mineral, the hyperfine splitting (HFS) constant A can be calculated from the position of the allowed HF line using the formula [14].

$$H_m = H_0 - Am - (35-4m^2)\left(\frac{A^2}{8H_0}\right).$$

Here H_m is the magnetic field corresponding to m ↔ m in HF line
H_0 is the resonance magnetic field.
m is the nuclear spin magnetic quantum number.

The value of A at room temperature is found to be 8.82(1) mT. Further the strength of the HFS depends on the matrix and is mainly determined by the electro negativity of the anion neighbours. The magnitude of the HFS constant, A provides a qualitative measure of the ionic nature of bonding between the Mn(II) ion. Using the hyperfine-coupling constant obtained from the EPR spectrum and with Matumura's plot [15], the percentage of covalency of Mn-ligand bond has been calculated. This corresponds to an ionicity of 93%

The percentage of covalency of Mn-O bond is calculated with their electronagativities X_P and X_q [16]

$$C = \frac{1}{n}\left[1 - 0.16\left(X_p - X_q\right) - 0.035\left(X_p - X_q\right)^2\right]$$

Here n is the number of ligands around Mn(II) ion. The percentage of covalency obtained is 8.5% assuming $X_p = X_{Mn} = 1.4$ and $X_q = X_S = 3.5$. Again the approximate value of hyperfine constant (A) is calculated by using covalency (C) using the equations [16,17]

$A_{iso} = (2.04C - 104.5)\ 10^{-4}\ cm^{-1}$.

The value obtained is 87 x 10^{-4} cm^{-1}. This calculated value agrees well with the observed hyperfine constant (87 x 10^{-4} cm^{-1}) indicating ionic character for Mn-O bond in the complex under study. Further the g value for the hyperfine splitting was indicative of the nature of bonding. If the g value shows negative shift with respect to free electron g value (2.0023), the bonding is ionic and conversely, if the shift is positive then the bonding is more covalent in nature [18]. In the present work, from the observed negative (2.00-2.0023 = -0.0023) shift in the g value, it is apparent that the Mn(II) is in an ionic environment.

3.2. Optical absorption spectral analysis

Optical absorption spectra of apjohnite in the range 50000-11110 cm^{-1} (200-900 nm) and 8700-8000 cm^{-1} are shown in Figs. 3a and b. The spectra discussed here have all the features that appear due to various electronic transitions involving manganese and iron. The observations are in tune with the chemical analysis. The spectra of the sample observed here have bands at 8482, 8288 (with a shoulder at 8116), 11975, 22730, 25640, 27780, 33900 and 45455 cm^{-1}. These bands are divided into two sets for easy analysis as 8482, 8288 (with a shoulder at 8116) and 11975 cm^{-1} (835 nm) as first set and 22730, 25640, 27780, 33900 and 45455 cm^{-1} (440, 390, 360, 295 and 220 nm) as second set in the sample. The bands in the second set correspond to the Mn(II) ion. The observed bands have been assigned to the d-d transitions of the d^5 ion having ground state $^6A_{1g}(S)$ following Tanabe-Sugano diagrams [19]. In a lower symmetry environment, the Mn(II) ion exhibits bands corresponding to the transitions from the ground state $^6A_{1g}(S)$ to $^4T_{1g}(G)$, $^4T_{2g}(G)$, $^4A_{1g}(G)$, $^4E_g(G)$, $^4T_{2g}(D)$, $^4E_g(D)$ and $^4T_{1g}(P)$ states respectively with increasing order of energy [20]. Assignment of each band to an appropriate electronic transition is difficult due to complexity of the transitions and multiplicity and distortions of the sites occupied by the transition metal ion. Therefore the energy matrices for d^5 configuration are solved for different Dq, B and C with Trees's correction term. The following values give best fit to the observed energies of the bands. Dq= 600, B=900 and C=3290 cm^{-1} and $\propto$ = 90 cm^{-1}. Observed and calculated values energies of the transitions for Mn(II) in octahedral site in the sample are presented in Table 1.

The first set of bands are characteristic of Fe(III) and Fe(II) ions occupying octahedral environment in the mineral (see below). The only spin allowed transition, $^5T_{2g} \rightarrow {}^5E_g$ which shows a strong band for all ferrous ion complexes [21,22] in the region 11000-8000 cm^{-1}. The two observed bands (Fig. 3b) centered around 8400 cm^{-1} are broad and intense assigned as two components of the same transition $^5T_{2g} \rightarrow {}^5E_g$ and the average of these bands (8482 and 8288 cm^{-1}) i.e. 8385 $cm^{-1}$is taken as 10Dq. The splitting of 10Dq band (8482 – 8288 = 194 cm^{-1}) indicates that it is due to dynamic Jahn-Teller effect in the excited ^5E_g state since the splitting value is an intermediate between 100 and 2000 cm^{-1}[23,24]. In many of the iron bearing silicates [25] and Mn-bearing zoisite [26] a broad band in the range 13000-11000 cm^{-1} has been observed and assigned to $^6A_{1g}(S)$ to $^4T_{1g}(G)$ transition for ferric ion. A broad weak band observed in apjohnite mineral at 11975 cm^{-1} could be due to Fe(III) impurity in the mineral. Sharp strong bands in the optical spectrum around 400 nm provide valid evidence for the presence of Mn^{2+} ion in the mineral. This result is in harmony with the EPR results. The mineral is white which is unusual for a mineral containing Mn^{2+}.

3.3. Near-infrared and infrared spectroscopy

The Near–IR spectral regions may be conveniently divided into three regions (a) the high wavenumber region > 7500 cm^{-1}. In this region electronic bands due to characteristic of Fe^{2+} and Fe^{3+} ions are observed. Bands in the spectrum shown in Fig.4a, the high wavenumber region between 7200 and 6300 cm^{-1} are attributed to the first overtone of the fundamental hydroxyl stretching mode. The 6000-4200 region spectrum shown in Fig.4b, where the bands in the range 6000- 5500 cm^{-1} are attributed to water combination modes of the hydroxyl fundamentals of water and the bands in the lower range 5500-4200 cm^{-1} are assigned to the combination of the stretching and deformation modes of the apjohnite. The mid-IR spectra as studied, may also be subdivided into four spectral regions: (a) 3700 to 2500 cm^{-1} region where OH fundamental vibrations are observed (Fig.5a); (b) 1800 to 1400 cm^{-1} range where the water bending modes are observed (Fig. 5b); (c) 1200 to 800 cm^{-1} region shows bands due S-O stretching vibrations (Fig. 5c) and (d) the low wavenumber region (700-645 cm^{-1}) displays a single mode for $(SO_4)^{2-}$ (Fig. 5d). As Raman spectroscopy of apjohnite has already been reported [1], the analysis are not discussed here. The results of the NIR spectra are given in Table 2 and the results of the mid-IR spectra in Table 3.

The 3700 to 2500 cm^{-1} spectral region

The OH stretching region of apjohnite is shown in Fig. 5a. The IR spectrum shows five bands at 3512, 3397, 3334, 3253 and 3112 cm^{-1}. The first two bands are assigned to OH stretching vibrations of water (ν_3) where as the bands at 3334, 3253 and 3112 $cm^{-1}$are identified as ν_1 mode of H_2O. In this region Raman spectrum (Fig. 6a) also displays almost similar band positions at 3496, 3406, 3337 and 3252 of which 3406 cm^{-1}band is most intense and sharp.

The 1800 to 1400 cm^{-1} spectral region

This region is significant for the observation of H_2O bending modes. The ν_2 water-bending modes are very weak in Raman but they more pronounced in the IR spectrum (Fig. 5b). A broad band profile centered at ~1600 cm^{-1} from which four bands are resolved at 1681, 1639, 1619 and 1517 cm^{-1}. From this group of bands, two bands are sharp and strong at 1681 and 1619 cm^{-1} with a shoulder at1639 cm^{-1}. The appearance of ν_2 mode on the higher wavenumber side at 1681 cm^{-1} is an indication of strongly hydrogen bonded water and the 1619 cm^{-1}mode to weakly hydrogen bonded water. This complexity of bands provides evidence for the existence of water in several states in the structure of apjohnite. The observation of four HOH bending modes is in harmony with the observation of four OH stretching modes in the Raman spectrum and five OH stretching vibrations ion the infrared spectrum.

The 1200 to 600 cm^{-1} spectral region

The infrared spectra for the fundamental vibrations of $(SO_4)^{2-}$ in the apjohnite mineral are shown in Figs. 5c and d. All the spectral features in this region are characteristic of sulphate groups. The free $(SO_4)^{2-}$on has ideal tetrahedral (T_d) symmetry and gives four fundamental vibrations at 981 (ν_1), 451(ν_2), 1104 (ν_3), 613(ν_4) cm^{-1}. Of these, ν_1 mode is non-degenerate, ν_2 mode is doubly degenerate and ν_3 and ν_4 modes are triply degenerate. In solid sulphate compounds the degeneracies are often removed by lowering of symmetry imposed by the molecular environment [27,28]. For ideal tetrahedral (T_d) symmetry all modes are Raman active while ν_1 and ν_2 are IR inactive. For pseudo-alums, the symmetry is lowered and all vibrations become active. In the present investigation, the most intense complex band around 1100 cm^{-1} resolved into a number of bands both in IR and Raman spectra (Figs. 5c and 6b) are assigned to the ν_3 $(SO_4)^{2-}$ antisymmetric stretching vibrations. The shoulder band at 982 cm^{-1} is attributed to the ν_1 $(SO_4)^{2-}$ symmetric stretching vibrations. A single broad band in IR at 667 cm^{-1} (Fig. 5d) is identified as the ν_4 mode. The ν_2 $(SO_4)^{2}$- bending modes are not observed in IR as they occur below the cut-off point for the diamond ATR cell. However, this mode could be observed at 496cm^{-1} in Raman (Fig. 6c). Bishop and Murad reported bands for both the synthetic and natural minerals at 663 and 630 cm^{-1} [29]. The analysis of IR and Raman spectra of apjohnite is presented in Table 3 along with the Raman data reported on Mn-bearing alum and also compared with that of Fe-bearing alums from three different origins. The OH region bands (3500-3100 cm^{-1}) observed both in IR and Raman agree closely with the Raman data already reported for apjohnite. One additional band observed in IR at 3122 cm^{-1} is assigned to OH stretch ν_1 H_2O. In the case of Fe^{2+} alums bands in this region are observed but shifted to higher wavenumber side. Since OH region bands are so sensitive, Mn and Fe alums could readily be differentiated. Such distinction is important for the detection of pseudo-alums in sulphate efflorescent deposits as occurs in mineral slag deposits. From the study of IR spectra, sharp bands at ~320 cm^{-1} have been reported for Mn^{2+} and Fe^{2+} in complexes with $M-O_6$ coordination [30]. The low energy Raman bands in the range 400-360 cm^{-1} observed for these alums are attributable to Mn-O/Fe-O vibrations.

4. Conclusions

1. Chemical analysis of the apjohnite mineral indicated that it contains manganese

0.64 and iron 0.06 wt% in the mineral as is verified by the spectroscopic analyses reported in this paper..

2. EPR results show that only Mn(II) is present in the mineral in distorted octahedral environment. The g and A values observed in the spectrum are 2.0 and 8.82 mT with D = 33 mT. The percentage of covalency obtained is 8.5%. The observed and calculated A values are in good agreement.
3. The optical absorption indicates that Mn(II) ion in the sample is present in a distorted octahedral environment. The crystal field and Racah parameters evaluated are Dq= 600, B= 900 and C =3290 $cm^{-1}$and $\propto$ = 90 cm^{-1}. Further the spectrum indicating that iron is present in +2 state in the sample.
4. The Infrared spectrum of apjohnite is assigned to fundamentals of water molecules and sulphate ions.
5. The Raman spectrum of apjohnite is compared with published data and is almost identical.

Acknowledgements

The financial and infra-structure support of the Queensland University of Technology (QUT), Inorganic Materials Research Program is gratefully acknowledged. One of us (SLR) is thankful to UGC, New Delhi for financial assistance (project link no: 1361, March 2004). One of the authors (B. J. R) is grateful to The Queensland University of Technology for the award of a Visiting Professorial Fellowship.

References

[1] R.L. Frost, J.T. Kloprogge, P.A.Williams. P.A., P. Leverett, J. Raman Spectrosc. 31 (2000) 1083.
[2] J.A. Anthony, R.A. Bideaux, K.W. Bladh, M.C. Nichols, "Hand Book of Mineralogy, Vol. V, Mineral Data Publishing, Tucson, Arizona, 2003, p. 29.
[3] S. Menchotti, C. Sabelli, Mineral. Mag. 40 (1976) 599.
[4] L.W. Lawrence, V. Munro-Smith, J. Proc. Roy. Soc. New South Wales 132 (1999) 29.
[5] I.L. Reinitz, G.R. Rossman, Am. Mineral. 73 (1988) 822.
[6] A. Ertl, J.M. Hughes, S. Prowatke, G.R. Rossman, D. London, E.A. Fritz, Am. Mineral. 88 (2003) 1369.
[7] S.D. Ross, Chapter 18 pp 423 in: The infrared spectra of minerals, V.C. Farmer editor, The Mineralogical Society London, 1974.
[8] S.D. Ross, Inorganic Infrared and Raman Spectra, McGraw-Hill Book Company Ltd, London, 1972.
[9] J. K. Beattie, S.P. Best, Coordination Chemistry Reviews 166 (1997) 391.
[10] A.J. Berry, B.D. Cole, R.S. Armstrong, J. of Raman Spectrosc. 30 (1999) 73.
[11] B.J. Reddy, R. L. Frost, W. N. Martens, Mineral. Mag. 69 (2005) 155.
[12] R.L. Frost, R. L., M.L. Weier, J.T. Kloprogge, J. Raman Spectrosc. 34 (2003) 776.
[13] R.L. Frost, R.L. Weier, Thermochim. Acta 409 (2004) 79.
[14] J.R. Pilbrow, Transition Ion Electron Paramagnetic Resonance, Clarendon Press, Oxford, UK, 1990.
[15] O. Matumura, J. Phys. Soc. Japan 14 (1959) 108.
[16] E. Simanck, K.A. Muller, J. Phys. Chem. Solids 31 (1970) 1027.
[17] A.M.F. Benial, V.Ramakrishnan, R.Kurugesan, Spectrochim. Acta A 55 (1999) 2573.
[18] V. Wieringen, Discuss. Faraday Soc. 19 (1955)118.
[19] Y. Tanabe, S. Sugano, J. Phys. Soc. Japan 9 (1953)753.
[20] A.B.P. Lever, Inorganic Electronic Spectroscopy, Elsevier, Amsterdam, 1984.
[21] G.R. Rossman, M.N. Taran, Am. Mineral. 86 (2001) 896.
[22] R.L. Frost, R.A. Wills, W.N. Martens, M.L. Weier, B. Jagannadha Reddy, Spectrochim. Acta, 62A ((2005) 42.
[23] G.H. Faye, Can. J. Earth. Sci. 5 (1968)3.
[24] W.Low, M.Weger, Phys. Rev. B 118 (1960) 1130.
[25] G.R. Rossman, Mineral. Spectrosc. 5 (1996) 23.
[26] G.Srinivasulu, B.Madhsudhana, B.J.Reddy, R.Natarajan, P.S.Rao, Spectrochim. Acta A 48 (1992)1421.
[27] H.H. Adler, P.F. Kerr, Am. Mineral. 50 132 (1965) 132.
[28] A. Hezel, S.D. Ross, Spectrochim. Acta A, 22 (1966) 547.
[29] A.J. Berry, B.D. Cole, R.S. Armstrong, J. of Raman Spectrosc. 30 (1999) 73.
[30] A.N. Lazarev, Vibrational spectra and structure of silicates. Consultants Bureau, New York, 1972.
[31] W.P. Griffith, in: Spectroscopy of Inorganic-based Materials, R.J.H. Clark, R.E. Hester, John Wiley & Sons, London, 1987, p. 119.

Table 1

Band headed data with the assignments for Mn(II) in apjohnite

Dq= 600, B= 900 and C =3290 $cm^{-1}$and $\propto$ = 90 cm^{-1}

Wavelength (nm)	Wave number (cm^{-1})		Transition from $^6A_{1g}$
	Observed	Calculated	
835*	11975*		$^4T_{1g}(G)$*
440	22730	22689	$^4T_{1g}(G)$
390	25640	26176	$^4T_{2g}(G)$
360	27780	27250	$^4A_{1g}(G)$, $^4E_g(G)$
295	33900	32322	$^4E_g(D)$
220	45455	44384	$^4T_{1g}(P)$

* Due to Fe^{3+} ion

Table 2
Analysis of the near-infrared bands in apjohnite

Band position (cm^{-1})	Assignment
8482*	Fe^{2+} transition: $^5T_{2g} \rightarrow {}^5E_g$
8288*	”
8116sh	”
6917	First fundamental overtone of OH stretch
6769c	”
6495c	”
5725	Water OH overtones
5610c	”
5150	”
5050c	”
4900c	”
4520	Combination of OH stretch and deformation

*average of the two bands represents Fe^{2+} transition
Sh-shoulder; c-component band

Table 3

IR and Raman spectroscopic data (cm^{-1}) of Mn and Fe bearing pseudo-alums from different origins

Apjohnite Mn^{2+}alum	Apjohnite Mn^{2+}alum	Apjohnite Mn^{2+}alum	Halotrichite Fe^{2+}alum	Halotrichite Fe^{2+}alum		Halotrichite Fe^{2+}alum	Assignments [7,31]
(Italy)	(Italy)	(Italy)	(Italy)	(Spain)		(California)	
Present work	Present work	Reported [1]	Unpublished Data by Frost	Unpublished Data by Frost		Unpublished Data by Frost	
IR	Raman	Raman	Raman	Raman	IR	IR	
3512	3496	3490	3452	3546	3538	3694	OH stretch ν_3 (B_g) H_2O
3397	3406	3394	3369	3425	3397	3573	OH stretch ν_3 (A_g) H_2O
3334	3337	3281	3255	3269	3228	3493	OH stretch ν_1 H_2O
3253	3252	3122	3166			3263	OH stretch ν_1 H_2O
3112						3031	OH stretch ν_1 H_2O
		2925	2944	2943		2873	Organic impurity
					2484	2501	“
1681		1658		1662	1650	1654	ν_2 (B_g) H_2O
1639		1620			1602	1604	ν_2 (A_g) H_2O
1619							ν_2 (A_g) H_2O
1517				1568			Combination band
					1453	1492	Combination band
1197	1198	1148	1148	1147	1134	1145	ν_3(A_g) SO_4
1138	1143	1113	1112		1105	1107	ν_3(B_g) SO_4
1105	1137	1088	1091	1084	1076	1075	ν_3(B_g) SO_4
1070	1117	1070	1070		1047		ν_3(B_g) SO_4
		1051	1053		988		ν_3(B_g) SO_4

982		997	995			1048	$\nu_1(A_g)$ SO_4
		991		988			$\nu_1(A_g)$ SO_4
						1017 (send up)	
		975	975	984	949	992	$\nu_1(A_g)$ SO_4
				983		949	$\nu_1(A_g)$ SO_4
				982		918	ν_L (A_g) H_2O
872						709	ν_L (B_g) H_2O
					717	626	$\nu_4(B_g)$ SO_4
	673			624			$\nu_1(A_g)$ AlO *
667	623	617	622	605	587	580	$\nu_4(B_g)$ SO_4
						570	$\nu_4(A_u)$ SO_4 or ν_T (B_g) H_2O
	505	530	529				$\nu_2(A_g)$ SO_4
	496	466	468	467		495	$\nu_2(A_g)$ SO_4
		427	424	445			$\nu_2(A_g)$ SO_4
	417		390	422			$\nu_1(A_g)$ MnO or FeO *
				380			$\nu_1(A_g)$ FeO *
		336	347	362			$\nu_1(A_g)$ MnO or FeO *
		313	314			318	Lattice modes *
		264	267	245			“
				221			Lattice modes
				204			Lattice modes
				182			Lattice modes
				116			Lattice modes

* suggested assignment

List of Figures

Fig. 1. EPR spectrum of apjohnite mineral at RT (ν = 9.41236 GHz) from 80 mT to 580 mT

Fig. 2. EPR spectrum of apjohnite mineral at RT (ν = 9.41236 GHz) from 255 mT to 405 mT.

Fig. 3a. Optical spectrum of apjohnite

Fig. 3b. NIR spectrum of apjohnite in the 8700 to 8000 cm^{-1} region.

Fig. 4a. NIR spectrum of apjohnite in the 7000 to 6300 cm^{-1} region.

Fig. 4b. NIR spectrum of apjohnite in the 6000 to 4200 cm^{-1} region.

Fig. 5a. IR spectrum of apjohnite in the 3725 to 2525 cm^{-1} region.

Fig. 5b. IR spectrum of apjohnite in the 1800 to 1400 cm^{-1} region.

Fig. 5c. IR spectrum of apjohnite in the 1225 to 825 cm^{-1} region.

Fig. 5c. IR spectrum of apjohnite in the 690 to 645 cm^{-1} region.

Fig. 6a. Raman spectrum of apjohnite in the 3600 to 3200 cm^{-1} region.

Fig. 6b. Raman spectrum of apjohnite in the 1240 to 1100 cm^{-1} region.

Fig. 6c. Raman spectrum of apjohnite in the 700 to 400 cm^{-1} region.

List of Tables

Table 1 Band headed data with the assignments for Mn(II) in apjohnite

Table 2 Analysis of the near-infrared bands in apjohnite

Table 3 IR and Raman spectroscopic data (cm^{-1}) of Mn and Fe bearing pseudo-alums from different origins

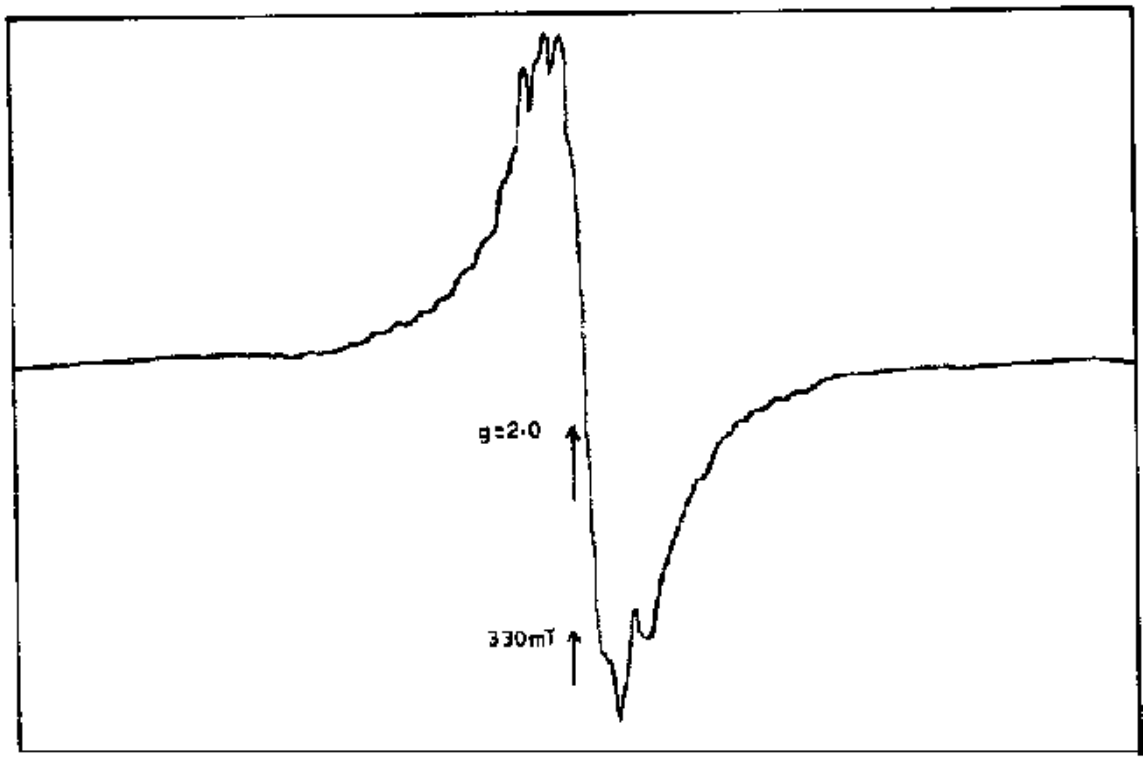

Fig.1 EPR spectrum of apjohnite mineral at RT (ν = 9.41236 GHz) from 80 mT to 580 mT

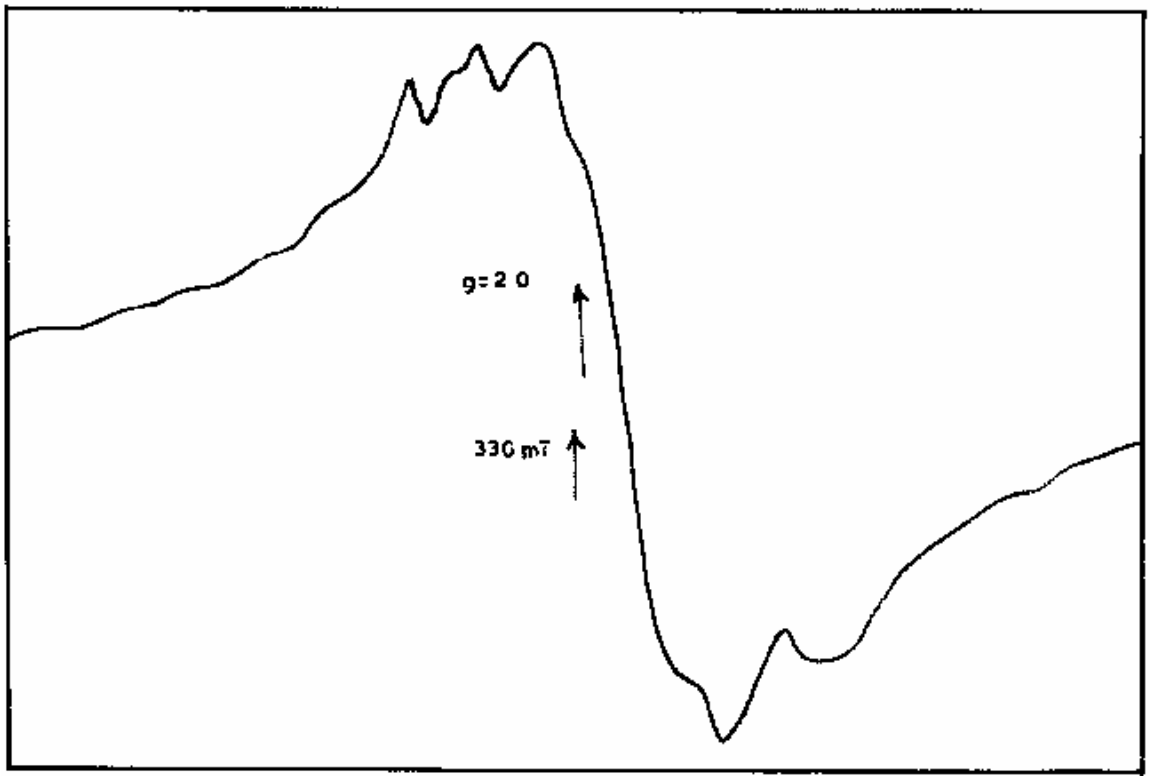

Fig.2 EPR spectrum of apjohnite mineral at RT (ν = 9.41236 GHz) from 255 mT to 405 mT.

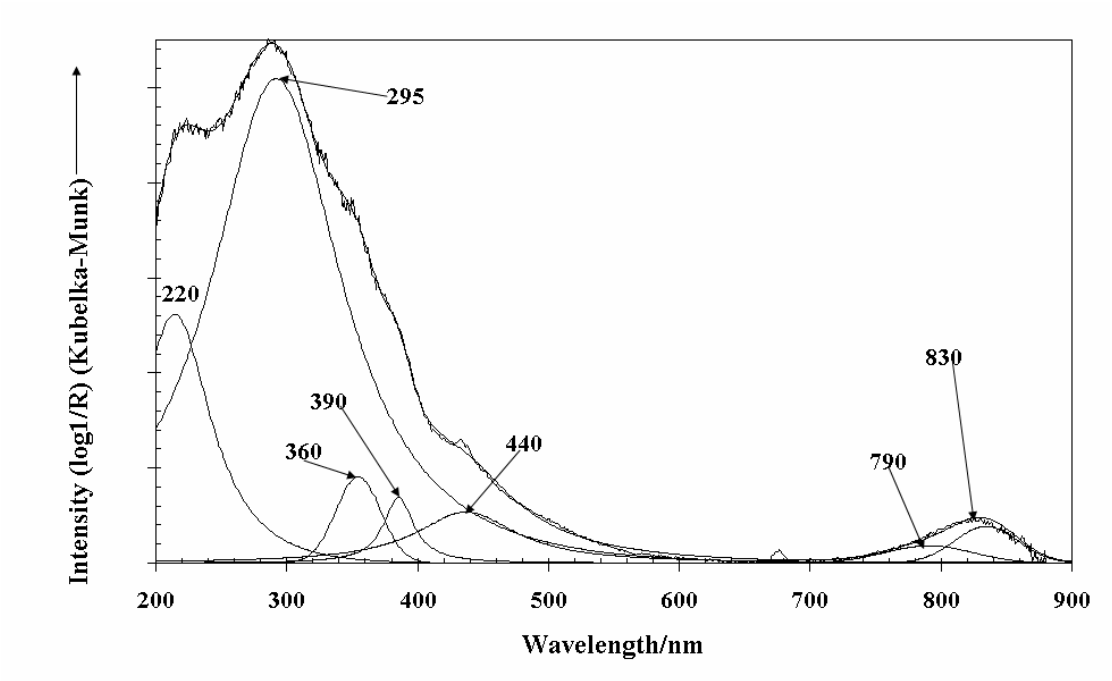
Intensity (log1/R) (Kubelka-Munk)
295
220
390
360
440
790
830
200
300
400
500
600
700
800
900
Wavelength/nm

Fig. 3a.

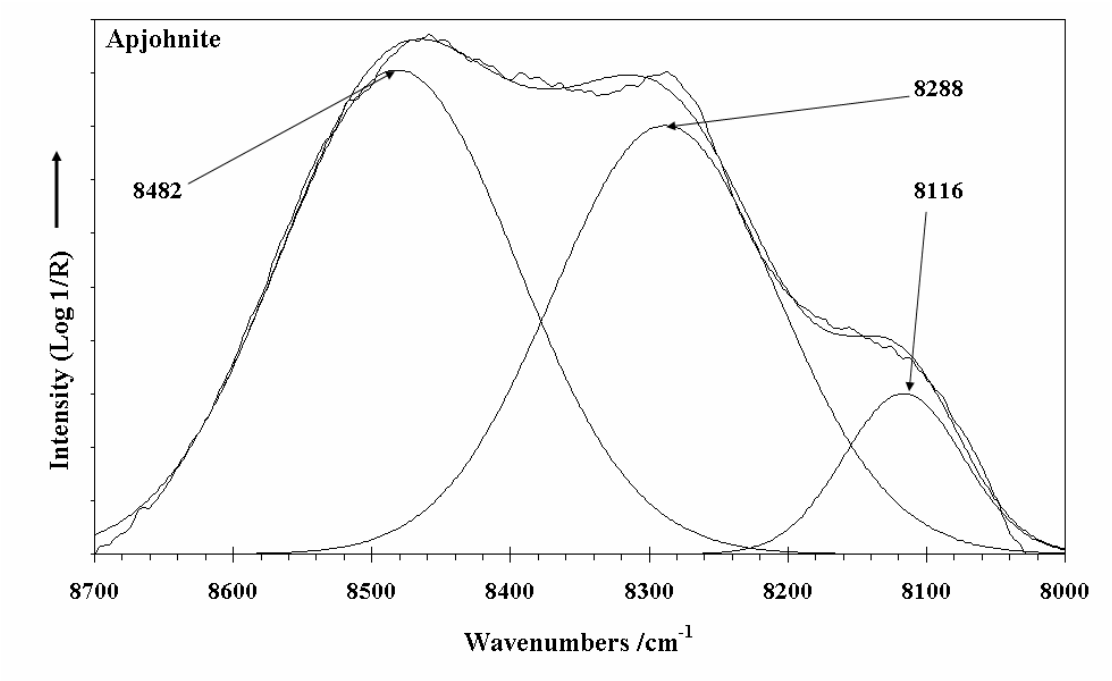
Apjohnite
8482
8288
8116
Intensity (Log 1/R)
8700
8600
8500
8400
8300
8200
8100
8000
Wavenumbers /cm-1

Fig. 3b.

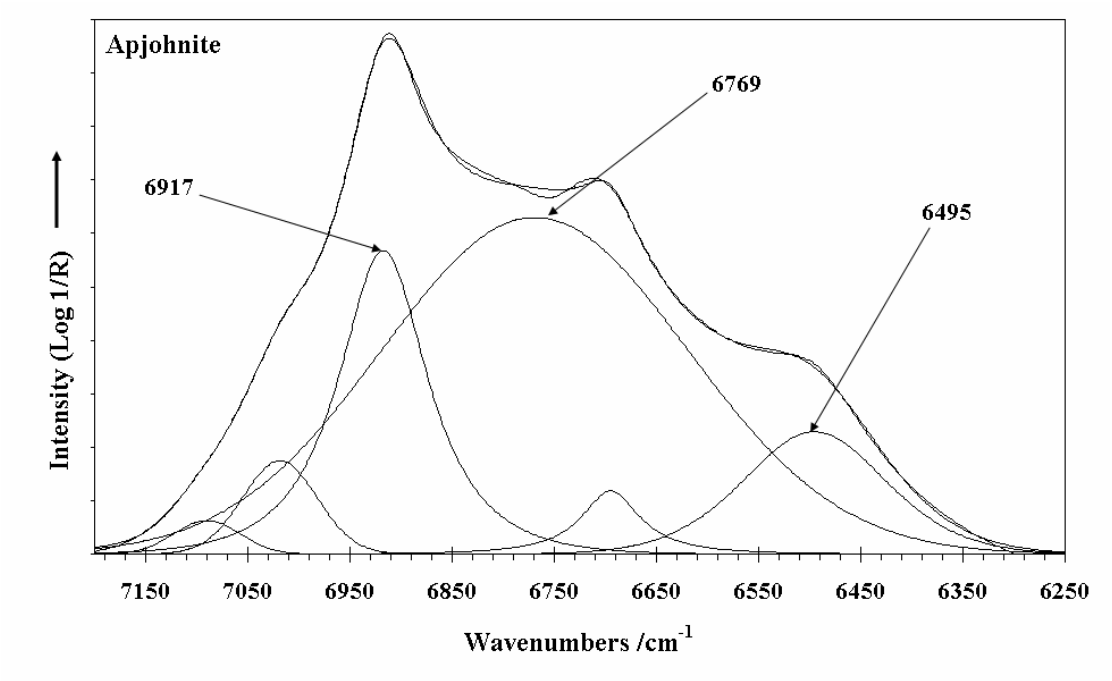
Apjohnite
6769
6917
6495
Intensity (Log 1/R)
7150
7050
6950
6850
6750
6650
6550
6450
6350
6250
Wavenumbers /cm-1

Fig. 4a

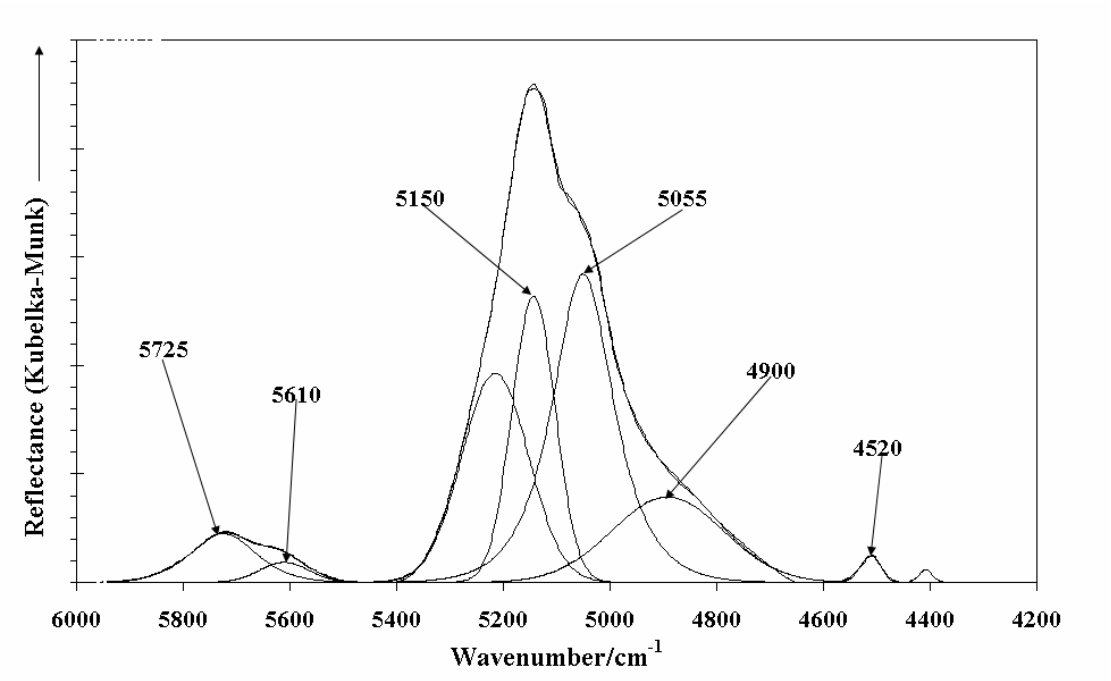
Reflectance (Kubelka-Munk)
5150
5055
5725
5610
4900
4520
6000
5800
5600
5400
5200
5000
4800
4600
4400
4200
Wavenumber/cm-1

Fig. 4b

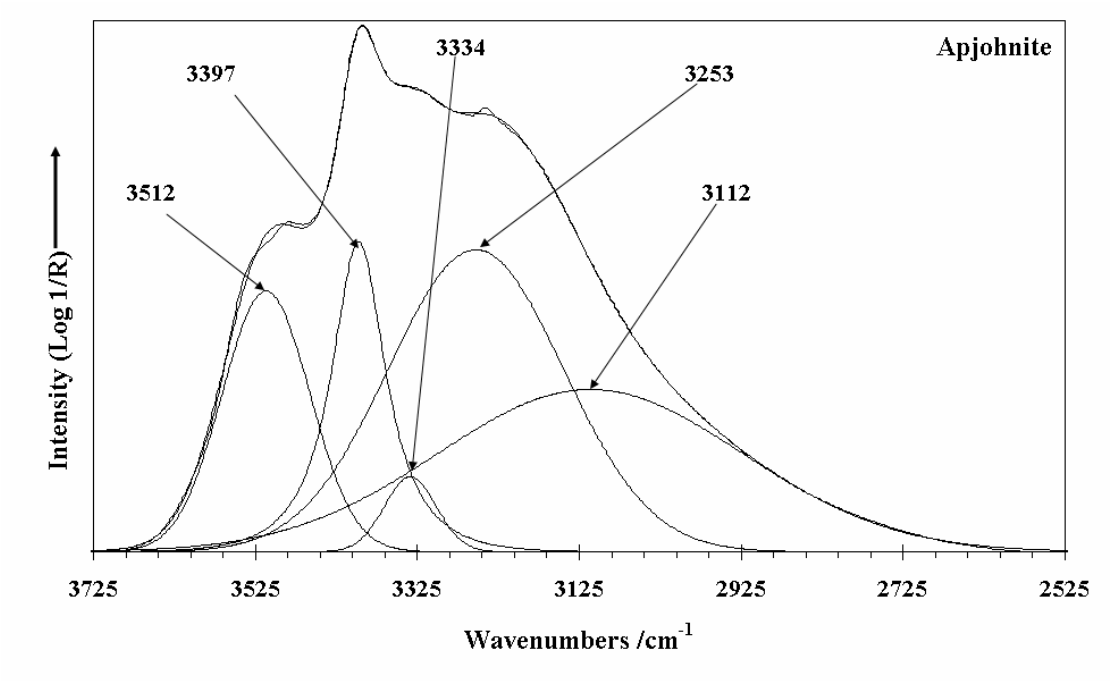
Apjohnite
3334
3397
3253
3512
3112
Intensity (Log 1/R)
3725
3525
3325
3125
2925
2725
2525
Wavenumbers /cm-1

Fig. 5a.

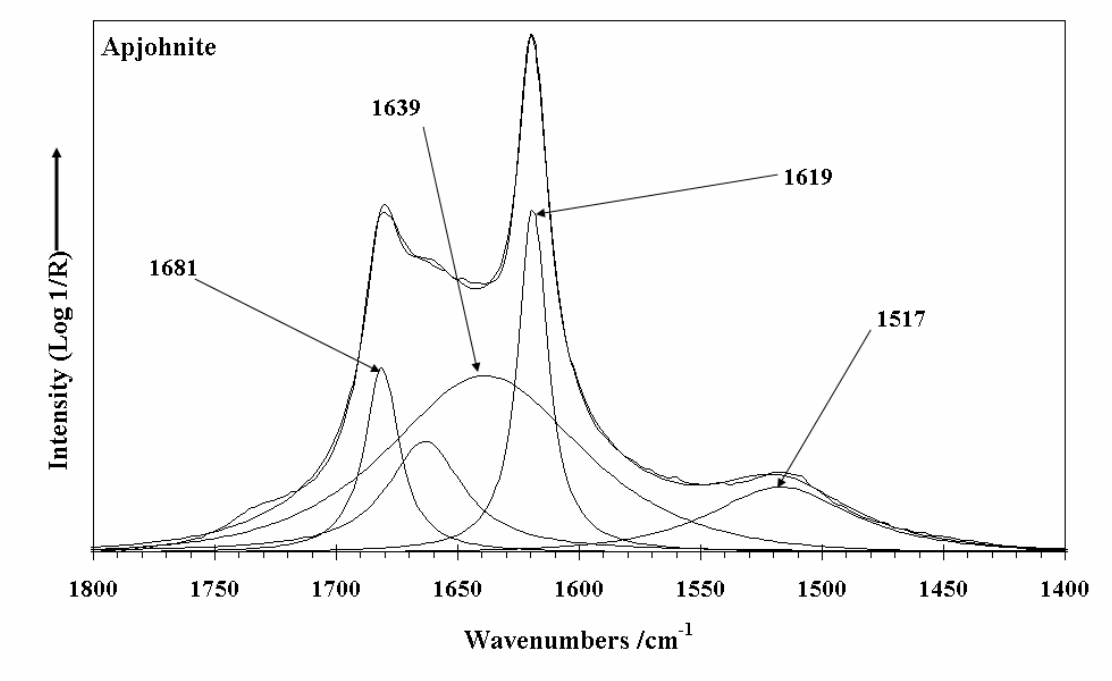
Apjohnite
1639
1619
1681
1517
Intensity (Log 1/R)
1800
1750
1700
1650
1600
1550
1500
1450
1400
Wavenumbers /cm-1

Fig.5b.

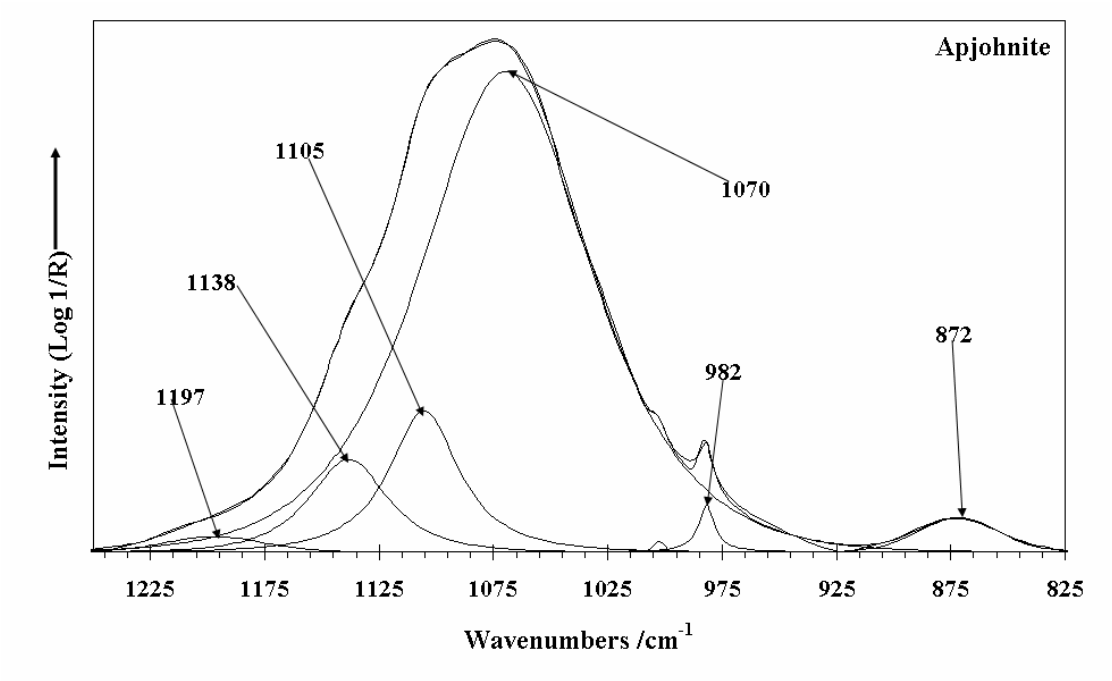
Apjohnite
1105
1070
1138
872
982
1197
Intensity (Log 1/R)
1225
1175
1125
1075
1025
975
925
875
825
Wavenumbers /cm-1

Fig. 5c.

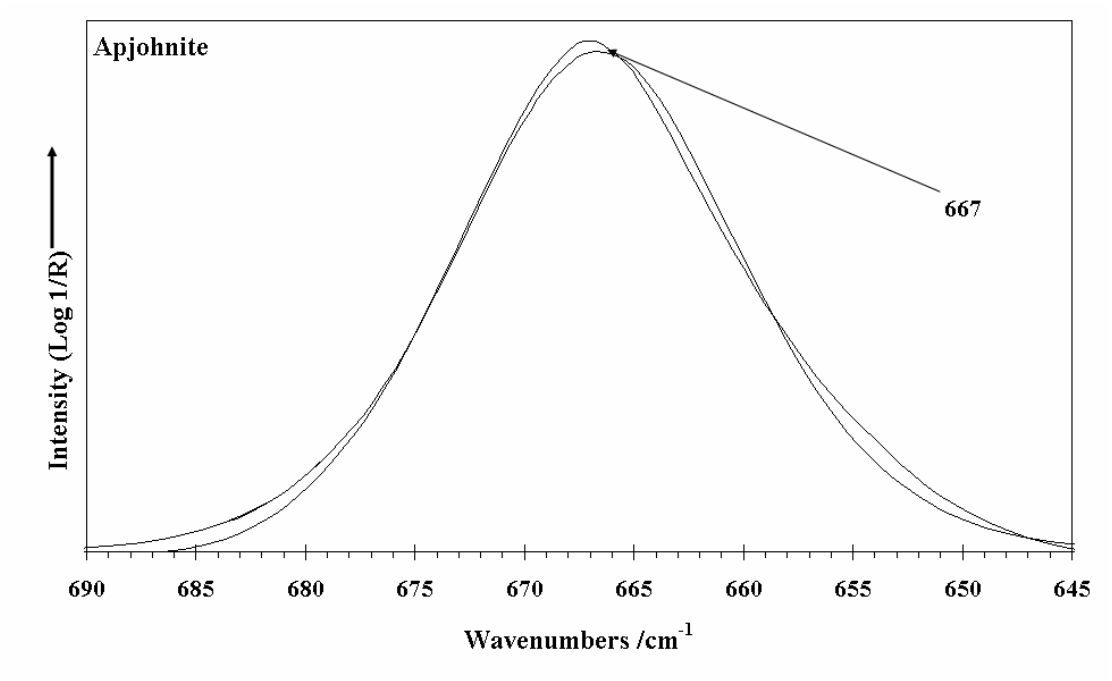
Apjohnite
667
Intensity (Log 1/R)
690
685
680
675
670
665
660
655
650
645
Wavenumbers /cm-1

Fig. 5d

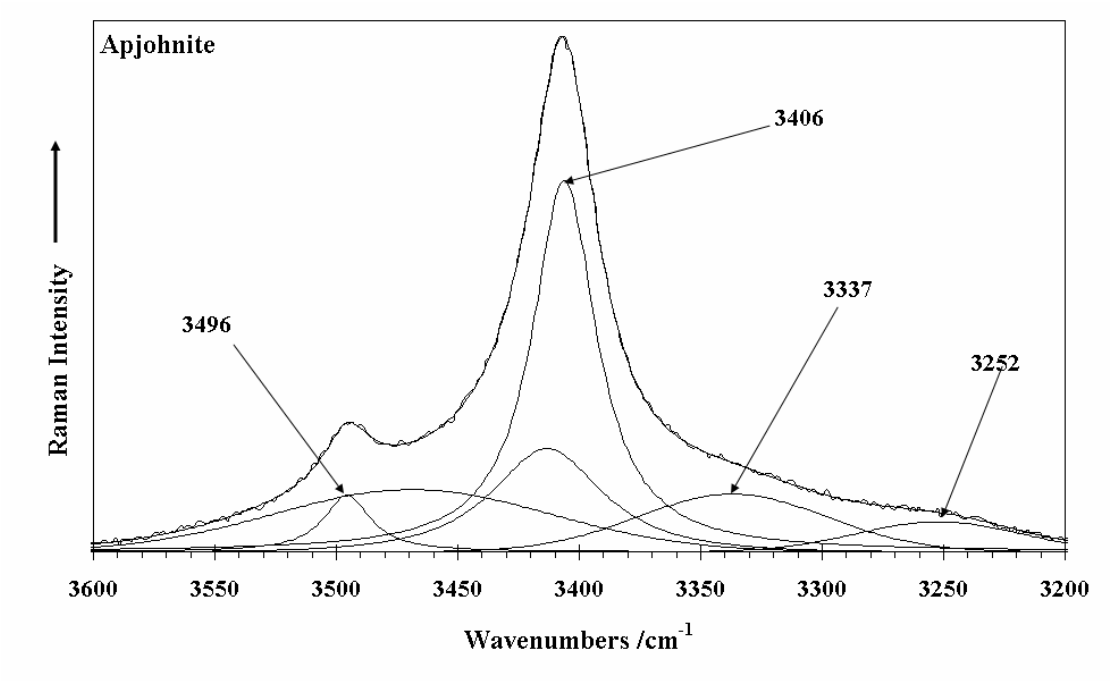
Apjohnite
3406
3337
3496
3252
Raman Intensity
3600
3550
3500
3450
3400
3350
3300
3250
3200
Wavenumbers /cm-1

Fig. 6a.

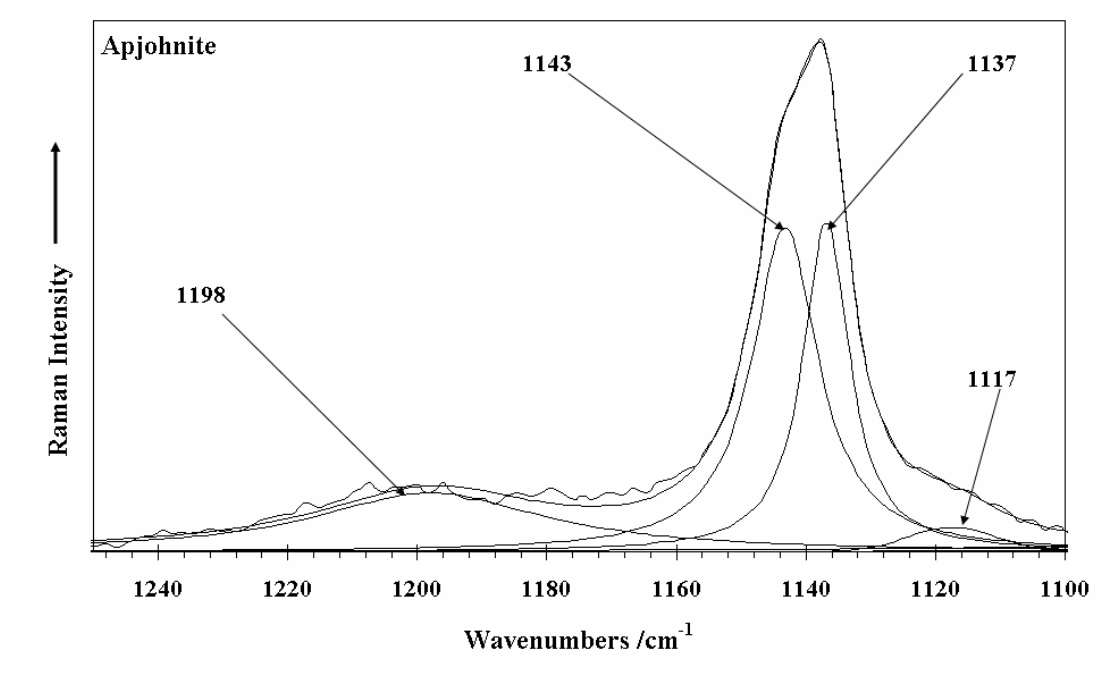
Apjohnite
1143
1137
1198
1117
Raman Intensity
1240
1220
1200
1180
1160
1140
1120
1100
Wavenumbers /cm-1

Fig. 6b

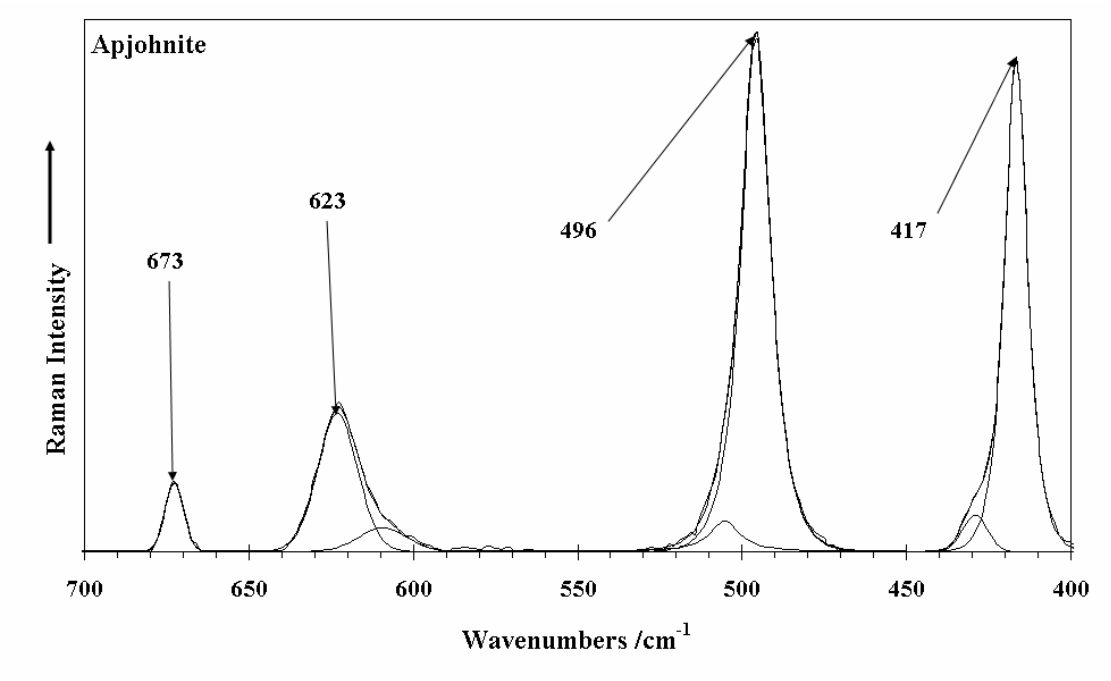
Apjohnite
673
623
496
417
Raman Intensity
700
650
600
550
500
450
400
Wavenumbers /cm-1

Fig. 6c.